Metallic and Semimetallic Silicon ⟨100⟩ Nanowires

R. Rurali and N. Lorente

Laboratoire Collisions, Agrégats, Réactivité, IRSAMC, Université Paul Sabatier, 118 route de Narbonne, 31062 Toulouse cédex, France

(Received 19 April 2004; published 20 January 2005)

Silicon nanowires grown along the ⟨100⟩ direction with a bulk Si core are studied with density-functional calculations. Two surface reconstructions prevail after exploration of a large fraction of the phase space of nanowire reconstructions. Despite their energetical equivalence, one of the reconstructions is found to be strongly metallic while the other one is semimetallic. This electronic-structure behavior is dictated by the particular surface states of each reconstruction. These results imply that doping is not required in order to obtain good conducting Si nanowires.

DOI: 10.1103/PhysRevLett.94.026805 PACS numbers: 73.22.–f, 81.07.Bc, 81.07.Lk

One-dimensional semiconductor nanostructures are attracting great interest for their potentially high impact in future molecular-electronics applications, such as nanoswitches and nanocontacts [1]. Silicon nanowires (SiNWs) appear to be an especially appealing choice, due to their ideal interface compatibility with conventional Si-based technology [2,3]. Moreover, measuring changes of their conductance allows us to use SiNWs as real-time label-free sensors in different chemical environments. The detection of NH_3 [4] and of biological macromolecules [5] has been reported, envisaging the possibility of reaching the single-molecule detection limit [6].

Recently, SiNWs of diameters below 10 nm have been synthesized. Ma *et al.* [7] have reported extremely thin SiNWs grown along the ⟨100⟩ lattice direction whose diameters range from 1.3 to 7 nm. Previously, Holmes *et al.* [8] obtained ⟨100⟩ and ⟨110⟩ SiNWs of 4 to 5 nm and discussed the influence of lattice orientation. Wu *et al.* [9] have grown ⟨110⟩, ⟨111⟩, and ⟨112⟩ SiNWs down to 3 nm. Colemann *et al.* [10] have reported SiNWs of 3 to 5 nm diameter.

Thus, a detailed understanding of the structure of thin SiNWs and of their mechanical and electrical properties as a result of the different growth conditions is required. While it has been extensively demonstrated that in H-terminated SiNWs, quantum confinement induces a gap-broadening effect [11–13], little is known about surface reconstruction of nonpassivated wires and about their electronic structure. Theoretical studies of the structure of the thinnest possible SiNWs [14,15] have been previously published. However, recent experiments have provided convincing evidence that some SiNWs grow around a monocrystalline bulk Si core [7,16]. Systems fulfilling such a requirement have been studied by Ismail-Beigi and Arias [17] [⟨100⟩ SiNWs] and by Zhao and Yakobson [18] [⟨100⟩ and ⟨110⟩ wires]. Both studies show the paramount importance of facet edges in wires with diameters in the nanometer range.

Thin nanowires pose fundamental problems with respect to their conduction properties. Recently, it has been discussed that doping may not be the advisable technique for tailoring nanodevice electrical properties because of the expected statistical deviation of impurity concentration from one system to another [13,19]. Indeed, typical concentrations for attaining the measured SiNWs conductance [20,21] may well mean that no donor or acceptor is actually present in nm-wide SiNWs. Some of these measurements show that conductance is larger than expected for doped SiNWs [20] and the authors suggest that surface states may be responsible for the measured conduction.

In this Letter, we present a theoretical study of realistic ⟨100⟩ SiNWs, with a bulk Si core and a diameter of $\sim$1.5 nm [17,18], thoroughly exploring the phase space of SiNW reconstructions. We study different periodic cells, ranging from 57 to 912 atoms, so that periodicity does not prevent us from finding the lowest-energy reconstruction. The mechanical properties of the SiNWs are studied by computing their Young modulus and Poisson ratio. Particularly, we focus our attention on the electronic properties of the wire as determined by the different possible lateral facet reconstructions. We give the first description of nanowire surface states as they evolve from the particular surface reconstruction of the studied SiNW. Depending on the reconstruction, the surface state can cross the Fermi level affecting the electrical characteristics of the nanowire. Hence, there is an intrinsic relation between the reconstruction of nanowire facets and its transport properties. This is a remarkable finding that shows that doping is not needed for obtaining conducting SiNWs.

We have performed density-functional theory (DFT) calculations with both a numerical atomic orbital [22] and a plane-wave [23] basis set. We have used a double-ζ polarized basis set [22] and a plane-wave energy cutoff of 20 Ry [23], with the generalized gradient approximation [24] for the exchange-correlation functional. We have studied wires in supercell geometry with a diameter of $\sim$1.5 nm. The axis periodicity will restrain the number of possible reconstructions and for this reason we have considered different supercell sizes, analyzing SiNWs of 57, 114, and 171 atoms. The reciprocal space has been sampled with a converged grid of 12, six, and four k points,

respectively. The atomic positions have been relaxed until the maximum force was smaller than 0.04 eV/Å.

The faceting geometry adopted by the wire is given by thermodynamical considerations [17,18,25]. On the one hand, the formation of {100} facets is favored over {110} facets, due the lower corresponding surface energy; on the other hand, facets with an even number of atoms can dimerize, lowering their energy, and are thus favored over facets with an odd number of atoms [26].

We have obtained two competing geometries for the {100} facets: a $1c$ reconstruction [see Fig. 1(a)] and a $2c$ reconstruction [see Fig. 1(b)], c being the lattice vector along the axis of the unreconstructed wire. The $1c$ reconstruction has the same periodicity of bulk Si, presents a *trough* in the middle of the facet, and turns out to be the most stable, with a cohesive energy of 3.990 eV/atom [27]. This value is only 3 meV/atom lower than for the $2c$ reconstruction. The small energy difference—probably within the accuracy of our calculations [28–30]—indicates that both reconstructions are likely to coexist. The trough in the $1c$ reconstruction is determined by the buckled dimer sequence, which presents a double chain of *low* atoms (labeled with a circle in Fig. 1); this rule is respected by only one of the two sides in the $2c$ reconstruction, while on the other side, one every two dimers is *flipped*. In contrast to what has been proposed for the Si(100) surface [32], none of the two cases shows spin polarization.

The two arrangements do not correspond to any infinite surface reconstruction, even though they loosely resemble the Si(100) $c(4 \times 2)$ and $p(4 \times 2)$ (but not the $p(2 \times 2)$; for the Si(100) surface reconstructions see, for example, Ref. [29]). The difference between surface and SiNW reconstructions stems from the lower coordination of the facet atoms. Between two adjacent dimers on the facet there is one single atom in the underneath layer, while between the corresponding dimers on the ⟨100⟩ surface there are two. This reduced coordination leads to a lateral shift of the dimers, increasing their packing.

In order to extensively explore other possible reconstructions, we have also performed nonorthogonal tight-binding (TB) [33,34] calculations, considering supercells

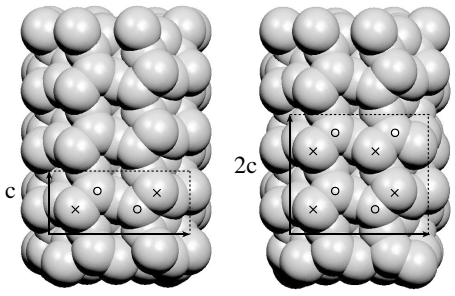

FIG. 1. {100}-facet reconstructions. (a) $1c$ and (b) $2c$ dimerization of the surface dangling bonds. Lattice vectors of the facet unit cell are sketched to underline the different periodicity along ⟨100⟩ axis (c is the bulk lattice parameter).

with a lattice parameter along the wire axis up to $16c$ (912 atoms). The TB structural relaxations are in very good agreement with the DFT results and no new reconstruction was found. We have also taken into account other faceting arrangements prior to relaxations, but we confirm that the minimum-energy configurations are obtained when {100} facets prevail [17,18,25]. Second-neighbor empirical potentials [35,36] have also been tested, but they have proven to be unsuitable to reproduce the complexity of these reconstructions.

Given the small energy difference between the two reconstructions, we have checked if at finite temperatures one of the two phases prevailed more clearly. We have calculated the Helmholtz free energy F following a quasiharmonic approach up to 300 K [37]. We have found that the difference between the two structures remains practically unchanged all over the temperature range analyzed. This is due to the fact that the vibrational contribution to F is determined by the integrated phonon density of states which hardly changes from one case to the other.

If SiNWs are to be used as nanoswitches or for manipulation purposes, it is important that they have a certain stiffness that prevents them from collapsing as a result of mechanical tensions. We have studied the response to axial stress in ⟨100⟩ SiNWs within nonorthogonal TB, finding a Young's modulus of ~137 GPa (~195 GPa for bulk Si) and a Poisson ratio of ~0.35 [38]. These values confirm the intuition that their bulk core make SiNWs mechanically stable.

We have calculated the band structure diagrams corresponding to the two different reconstructions. Surprisingly, the electronic structures turn out to be utterly different, especially if compared to their rather similar geometries. The $1c$ reconstruction has four clearly metallic states [see Fig. 2(a)], while the $2c$ wire shows a semimetallic behavior with a single Fermi-level crossing at the zone boundary [see Fig. 2(b)]. The metallic character of the $1c$ wire is robust against failures of DFT. A scissor operator correction would rigidly shift some of the electronic bands. In order to open a gap, both of the degenerate bands (ii) and (iii) in Fig. 2(a) should become fully occupied or fully empty because both bands have the same symmetry (see Fig. 3). Given the band structure about the Fermi energy, it is not possible to find shifts of other bands to prevent this shift from violating electron counting. Thus the $1c$ wire has metallic character. However, the limitations of DFT approximations to give the correct band gap of bulk silicon only permit to claim that the $2c$ wire is a semimetal of a small gap material.

The two reconstructions evince two competing mechanisms ruling the surface energetics in connection with the electronic structure of the SiNWs. There is a trade off between recovering the bulklike tetrahedral coordination on one side and the full delocalization of a genuine Bloch state along the wire axis on the other side. The first of these two mechanisms favors the flipping of one of the dimers, which is characteristic of the $2c$ reconstruction. The larger

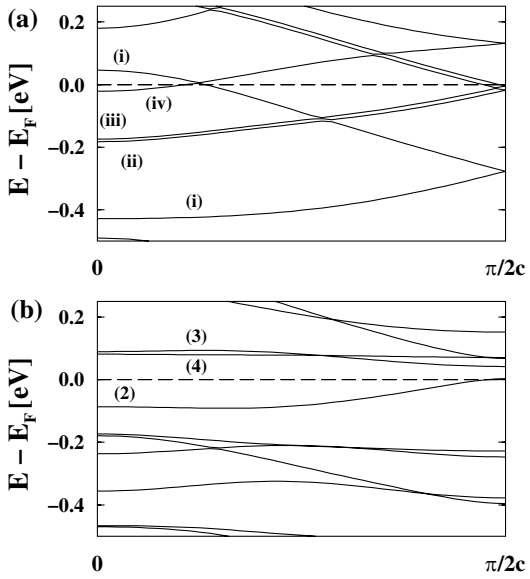

FIG. 2. Band structure diagrams. (a) The $1c$ reconstruction has four metallic states [(i) to (iv)] clearly crossing the Fermi level. (b) The $2c$ reconstruction has rather a single semimetallic state. For comparison, both diagrams refer to the $2c$ unit cell.

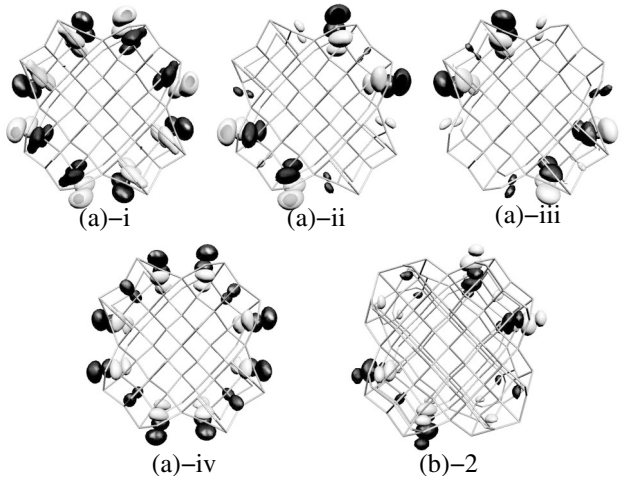

FIG. 3. Cross-section view of the wave functions at Γ point of (a) the four metallic states of the $1c$ reconstruction [(i) to (iv)] and (b) the semimetallic state of the $2c$ reconstruction. Labeling follows the scheme of Fig. 2. These wave functions give a false impression of C_{2v} symmetry. The *pseudo* C_{2v} symmetry explains why bands (ii) and (iii) are almost degenerate [surface states (a)-ii and (a)-iii in the figure].

coordination of the protruding Si atom in the flipped dimer leads to angles of $\sim 100°$, while the corresponding angles in the $1c$ reconstruction are of $\sim 90°$. This energy gain is compensated by the shift of the electronic structure as shown in Fig. 2. This shift is due to the reduction of symmetry by the flipped dimer. The flipped dimer interrupts the surface Bloch states, hence the overlap between dangling bonds is reduced in the $2c$ reconstruction and the energy of the surface states increases. Electronic localization induces an increase of energy by breaking the one-dimensional Bloch state, but on the other hand makes the system lower its energy locally by increasing the bonding of one of the dimers.

The bands of the $1c$ reconstruction can be identified with the $2c$-reconstruction ones, Fig. 2. The (ii) band of Fig. 2(a) shows similar symmetry as the (2) of Fig. 2(b) (see Fig. 3 below). An adiabatic calculation, slowly flipping the dimer yields this one-to-one correspondence. In the same manner, bands (iii) and (iv) of Fig. 2(a) can be identified with (4) and (3) of Fig. 2(b), respectively. The effect on the electronic structure of flipping one dimer is to localize, leading to higher-energy and flatter bands, Fig. 2(b).

The electronic structure about the Fermi energy is given by the surface states originating in the dimer dangling bonds. This is shown in Fig. 3. Isosurfaces of wave-function amplitude have been plotted on the SiNW atomic structure, showing that Bloch states originate on the facet dangling bonds. Figure 3 also shows the correspondence of the wave functions (a)-ii and (b)-2, as explained above. Surface states are thus present in both reconstructions.

Conductance through thin SiNWs remains a difficult issue [20]. The way SiNWs bind to metal electrodes is complex and crucial for determining the actual conductance of SiNW-based devices. In the absence of defects and in the case of excellent electrode contacts, the strongly metallic SiNW ($1c$-reconstructed) will present a maximal conductance of four quanta, equivalent to a resistance of only $\sim 3\ \mathrm{k}\Omega$ per SiNW. In the same conditions, the semimetallic SiNW ($2c$-reconstructed) exhibits a minimum resistance of $\sim 13\ \mathrm{k}\Omega$ per SiNW. These results show that SiNWs can be good conductors, and their actual electrical properties will be strongly dependent on the growth conditions. Experimental studies [20] show that despite diffusion from the metallic contacts and/or surface contamination, the measured conductance of thin SiNWs after annealing is much higher than the one expected from doping the SiNWs. This finding is in qualitative agreement with the above surface-state driven conduction.

Any perturbation on the surface states will drastically affect the conduction properties of the wires. These wires will be extremely sensitive to the chemical environment and therefore are good candidates for molecular detection [4–6].

In conclusion, we have performed DFT calculations allowing for different reconstructions of ⟨100⟩ SiNWs with a bulk core. The SiNWs are classified according to their {100}-facet reconstructions. No direct correspondence is found with infinite surface reconstructions, hence the two minimum-energy possibilities are classified according to the size of their periodicity along the wire axis: $1c$ for the one with the shortest period and $2c$ for the longest one. The bulklike core of the wire confers them with a Young modulus close to the bulk Si one; on the other hand, the Poisson ratio indicates good lateral elastic properties of these wires. Despite the closeness in energy of the two reconstructions, the $1c$ one shows a strong metallic

character while the $2c$ one is semimetallic. We have rationalized these findings in terms of the gain in energy due to the formation of surface-state versus tetrahedral-like angles in the surface dimers. Surface states are probably ubiquitous in a large family of SiNWs. The wires studied here present good conduction properties thanks to the reconstruction-induced surface states. Hence, the use of thin SiNWs as conductors without doping is possible.

R. R. acknowledges the financial support of the Generalitat de Catalunya. N. L. thanks ACI jeunes chercheurs. Computational resources at the Centre Informatique National de l'Enseignement Supérieur and the Centre de Calcul Midi-Pyrénées are gratefully acknowledged. We thank A. G. Borisov, E. Hernández, and P. Ordejón for their suggestions.

[1] D. Appell, Nature (London) **419**, 553 (2002); A. M. Morales and C. M. Lieber, Science **279**, 208 (1998); C. M. Lieber, Nano Lett. **2**, 81 (2002).
[2] Y. Huang, X. Duan, Y. Cui, L. J. Lauhon, K. Kim, and C. M. Lieber, Science **294**, 1317 (2001).
[3] L. J. Lauhon, M. S. Gudiksen, D. Wang, and C. M. Lieber, Nature (London) **420**, 57 (2002).
[4] X. T. Zhou, J. Q. Hu, C. P. Li, D. D. D. Ma, C. S. Lee, and S. T. Lee, Chem. Phys. Lett. **369**, 220 (2003).
[5] Y. Cui, Q. Wei, H. Park, and C. M. Lieber, Science **293**, 1289 (2001).
[6] J. Hahm and C. M. Lieber, Nano Lett. **4**, 51 (2004).
[7] D. D. D. Ma, C. S. Lee, F. C. K. Au, S. Y. Tong, and S. T. Lee, Science **299**, 1874 (2003).
[8] J. D. Holmes, K. P. Johnston, R. C. Doty, and B. A. Korgel, Science **287**, 1471 (2000).
[9] Y. Wu, Y. Cui, L. Huynh, C. J. Barrelet, D. C. Bell, and C. M. Lieber, Nano Lett. **4**, 433 (2004).
[10] N. R. B. Colemann, M. A. Morris, T. R. Spalding, and J. D. Holmes, J. Am. Chem. Soc. **123**, 187 (2001); N. R. B. Colemann, N. O'Sullivan, K. M. Ryan, T. A. Crowley, M. A. Morris, T. R. Spalding, D. C. Steytler, and J. D. Holmes, *ibid.***123**, 7010 (2001).
[11] B. Delley and E. F. Steigmeier, Appl. Phys. Lett. **67**, 2370 (1995).
[12] A. J. Read, R. J. Needs, K. J. Nash, L. T. Canham, P. D. J. Calcott, and A. Qteish, Phys. Rev. Lett. **69**, 1232 (1992).
[13] U. Landman, R. N. Barnett, A. G. Scherbakov, and P. Avouris, Phys. Rev. Lett. **85**, 1958 (2000).
[14] M. Menon and E. Richter, Phys. Rev. Lett. **83**, 792 (1999).
[15] B. X. Li, P. L. Cao, R. Q. Zhang, and S. T. Lee, Phys. Rev. B **65**, 125305 (2002).
[16] Y. F. Zhang, L. S. Liao, W. H. Chan, S. T. Lee, R. Sammynaiken, and T. K. Sham, Phys. Rev. B **61**, 8298 (2000).
[17] S. Ismail-Beigi and T. Arias, Phys. Rev. B **57**, 11923 (1998).
[18] Y. Zhao and B. I. Yakobson, Phys. Rev. Lett. **91**, 035501 (2003).
[19] F. G. Pikus and K. K. Likharev, Appl. Phys. Lett. **71**, 3661 (1997).
[20] J. Yu, S. Chung, and J. R. Heath, J. Phys. Chem. B **104**, 11864 (2000).
[21] Y. Cui, X. Duan, J. Hu, and C. M. Lieber, J. Phys. Chem. B **104**, 5113 (2000).
[22] J. M. Soler, E. Artacho, J. D. Gale, A. García, J. Junquera, P. Ordejón, and D. Sánchez-Portal, J. Phys. Condens. Matter **14**, 2745 (2002); Siesta: A Linear-Scaling Density-Functional Method, http://www.uam.es/siesta/.
[23] B. Hammer, L. B. Hansen, and J. K. Nørskov, Phys. Rev. B **59**, 7413 (1999); The Center for Atomic-Scale Materials Physics, http://www.fysik.dtu.dk/campos/.
[24] J. P. Perdew, K. Burke, and M. Ernzerhof, Phys. Rev. Lett. **77**, 3865 (1996).
[25] R. Rurali and N. Lorente, cond-mat/0412236.
[26] S. B. Zhang and S. H. Wei, Phys. Rev. Lett. **92**, 086102 (2004).
[27] We have obtained a value of 4.444 eV/atom for bulk Si.
[28] According to Ref. [29], a numerical uncertainty of a few meV per dimer is to be expected for the Si(100) surface DFT calculations. Our conclusion is then that given the numerical convergency attained in our calculations, the 3 meV/atom difference is significative. The GGA of Ref. [24] used in the present calculations gives correct geometries and accurate total energies for surfaces. In particular, recent studies of Si(100) show that the typical approximations of DFT give correct results in surface reconstruction and geometries (see Ref. [30]). Hence, the reconstructions presented here are probably within a few percent of the actual bond distances and angles. The metallicity of different Si surface reconstructions is reproduced by DFT calculations. Indeed, the metallic character of a given surface reconstruction has been used to predict and analyze the actual surface reconstructions of semiconductors; see, for example, Ref. [31].
[29] A. Ramstad, G. Brocks, and P. J. Kelly, Phys. Rev. B **51**, 14504 (1995).
[30] S. B. Healy, C. Filippi, P. Kratzer, E. Penev, and M. Scheffler, Phys. Rev. Lett. **87**, 016105 (2001).
[31] D. J. Chadi, Phys. Rev. Lett. **43**, 43 (1979); A. A. Stekolnikov, J. Furthmüller, and F. Bechstedt, Phys. Rev. B **65**, 115318 (2002).
[32] E. Artacho and F. Ynduráin, Phys. Rev. B **42**, 11310 (1990).
[33] D. Porezag, T. Frauenheim, T. Köhler, G. Seifert, and R. Kaschner, Phys. Rev. B **51**, 12947 (1995).
[34] R. Rurali and E. Hernández, Comput. Mater. Sci. **28**, 85 (2003).
[35] J. Tersoff, Phys. Rev. Lett. **56**, 632 (1986).
[36] J. F. Justo, M. Z. Bazant, E. Kaxiras, V. V. Bulatov, and S. Yip, Phys. Rev. B **58**, 2539 (1998).
[37] See, for instance, N. L. Allan *et al.*, Phys. Chem. Chem. Phys. **2**, 1099 (2000); this approximation has shown an excellent agreement with more accurate methods of free energy calculation [M. de Koning *et al.*, Phys. Rev. Lett. **83**, 3973 (1999)] up to 500 K [M. Kaczmarski *et al.*, Phys. Rev. B, **69**, 214105 (2004)].
[38] The Young's modulus is the ratio between stress and the axial strain ϵ and is conventionally defined as $Y = \frac{1}{V_0} \times \frac{\partial^2 E}{\partial \epsilon^2}|_{\epsilon=0}$, where V_0 and E are the equilibrium volume and the total energy, respectively; the Poisson ratio is defined as $\sigma = -\frac{1}{\epsilon}\frac{R-R_0}{R_0}$, where R_0 is the equilibrium radius of the SiNW and R is the radius at strain ϵ.